Composites Part C: Open Access 12 (2023) 100406

Contents lists available at ScienceDirect

Composites Part C: Open Access

journal homepage: www.sciencedirect.com/journal/composites-part-c-open-access

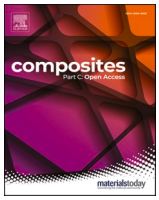

Biochar reinforced PLA composite for fused deposition modelling (FDM): A parametric study on mechanical performance

Prashant Anerao [a], Atul Kulkarni [a], Yashwant Munde [b,*], Avinash Shinde [b], Oisik Das [c,*]

[a] Department of Mechanical Engineering, Vishwakarma Institute of Information Technology, Pune 411046, India
[b] Department of Mechanical Engineering, Cummins College of Engineering for Women, Pune 411052, India
[c] Department of Civil, Environmental and Natural Resources Engineering, Lulea University of Technology, Lulea, Sweden

ARTICLE INFO

Keywords:
3D-printing
Biocomposite
Biochar
PLA polymer
Mechanical properties
Statistical analysis

ABSTRACT

Rice husk biochar was added to polylactic acid (PLA) to create a biocomposite filament suitable for the extrusion-based 3D printing process of fused deposition modelling (FDM). Taguchi L_{16} was used for experiment design, and the significance of process parameters was determined using variance analysis (ANOVA). For a 0.3-mm layer thickness, the addition of 5 wt.% biochar resulted in ultimate tensile strength and a modulus of elasticity of 36 MPa and 1103 MPa, respectively. The addition of biochar had a negative influence on flexural strength. The maximum flexural modulus was obtained with 3 % biochar, 100 % infill density, and 0.1 mm layer thickness. Particularly, 1 % biochar resulted in a considerable increase in impact strength, while a subsequent rise in biochar resulted in a decrease, probably due to the agglomeration effect. For 3D printed neat PLA, the average tensile strength, tensile modulus, flexural strength, flexural modulus, and impact strength observed were 19 MPa, 550 MPa, 54 MPa, 1981 MPa, and 25 KJ/m^2, respectively. Additionally, considering the output of each test, a multicriteria decision-making model, namely, TOPSIS, has been utilized for ranking the mechanical performance. In order to optimise the mechanical properties of three-dimensional printed objects, the study suggests a layer thickness of 0.2 mm, an infill density of 100 %, and raster angle of 0° as the FDM process parameters.

1. Introduction

Additive manufacturing, commonly referred to as 3D printing, has gained widespread popularity due to its ability to create complex geometries and customized products with ease and speed [1]. Among various 3D printing processes, Fused Deposition Modelling (FDM) is an extensively used and economical method for producing 3D parts. In FDM, molten polymer is extruded through a nozzle, which solidifies on cooling to form a 3D object, layer by layer. The technique offers significant design flexibility, low lead time, and cost-effective production. FDM printing technology predominantly employs thermoplastic polymers like Acrylonitrile Butadiene Styrene (ABS), Polylactic acid (PLA), Nylon, Polyethylene terephthalate glycol (PETG), and Thermoplastic Polyurethanes (TPU). These materials have been used in several applications, ranging from automotive to medical [2]. The selection of polymer material depends on the specific requirements of the printed part, such as strength, stiffness, and durability. However, the mechanical performance of the 3D printed items is often not satisfactory, limiting the application of 3D printing in high-performance engineering applications.

The physical and mechanical characteristics of 3D printed items depend largely on the filament material and process parameters like raster angle, layer thickness, nozzle temperature, bed temperature, infill density, and infill pattern. Rodriguez-Panes et al. [3] analysed the impact of build orientation, infill density and height of layer on mechanical behaviour in PLA and ABS. The results of the investigation demonstrated that PLA had a greater influence on the variations in process parameters compared to ABS. The investigation by Chokshi et al. [4] revealed that the choice of infill density and pattern affects the strength of specimens produced by FDM significantly. Infill density and thickness of the layer have a notable impact on the ability of the printed samples to withstand bending forces; the flexural strength (112 MPa) increased five times at optimised FDM process parameters. Mensah et al. [5] found that at higher infill density, 3D-printed PLA had better tensile and ductile properties and enhanced fire properties.

To overcome the limitations of polymer materials, researchers have explored the use of fibre reinforcement to enhance the mechanical properties of FDM printed parts. Both synthetic and natural fibres have

* Corresponding authors.
E-mail addresses: yashwant.munde@gmail.com (Y. Munde), oisik.das@ltu.se (O. Das).

https://doi.org/10.1016/j.jcomc.2023.100406

Available online 23 September 2023

Table 1
Physical and mechanical properties of PLA materials as provided by the supplier.

Matrix	Melt flow index (g/10 min)	Density (g/cc)	Tensile modulus (MPa)	Tensile strength (MPa)	Elongation at yield (%)
PLA: 3D850	7–9	1.24	2315	50	3.31

been investigated as potential reinforcements. The utilization of High Strength High Temperature (HSHT) fibreglass as reinforcement in the 3D printing process resulted in a 56 % increase in impact strength compared to conventional FDM materials. However, it was observed that there is a limit to the amount of HSHT fibreglass that can be added, which is 59 % by volume, before reaching an extent where further increments actually reduce the impact strength [6]. Synthetic fibres are derived from non-renewable resources and have a considerable ecological footprint. Alternative reinforcement options, such as natural fibres or bio-based materials, which offer comparable strength characteristics while being more environmentally friendly, are being explored. Natural fibres have attracted attention due to their low cost, renewable nature, and sustainability. Natural fibres like hemp [7], jute [8], and flax [9] have been used as reinforcement in FDM printed parts, with varying degrees of success. The use of agricultural residues as fillers in PLA (Polylactic Acid) has shown a significant improvement in the thermo-mechanical properties of the resulting composite after 3D printing [10].

Another promising additive to FDM printing is biochar, a carbon-rich product derived from the pyrolysis of organic waste. Biochar is a renewable material with a multitude of positive environmental impacts as well as possessing unique inherent properties [11]. The use of biochar in polymer composites has been identified as a possible technique to enhance sustainability [12–14]. This is supported by a study conducted by Kane and Ryan, indicating a substantial increase in the rate of degradation of PLA with biochar in composting environments as compared to neat PLA samples [15]. To enhance the thermal and mechanical characteristics of polymer composites, biochar is being used as a reinforcement material. In the study by Huang et al., it was demonstrated that the incorporation of grapevine biochar in PLA led to significant improvements in the tensile and impact strengths of the composite, with increases of 41.4 % and 32.1 %, respectively, compared to pristine PLA [16]. Tensile modulus was improved after the addition of 5 % biochar by weight to the hemp/PLA composite [17]. When 40 % biochar was added to rHDPE (recycled high-density polyethylene), tensile strength, stiffness, and flexural storage modulus improved significantly but the composite became too brittle [18]. Pudełko et al. discovered enhancements in the thermo-mechanical properties of composites when sewage sludge-derived biochar was incorporated into PLA (polylactic acid) [19]. At 25 % loading by weight, the addition of carbon-rich biochar (CRB) produced from agricultural by-products increased the tensile modulus by 21 % and the impact strength by 76 % for the CRB/PLA composite [20]. Zhang et al. [21] observed that at a high content, i.e., 70 wt.% of biochar derived from poplar wood in the high-density polyethylene, the stress concentration was very high, resulting in a 50 % decrease in flexural strength. This study suggests the characteristics of biochar/polymer composites are largely influenced by the amount of filler used.

Research has shown that biochar-reinforced polymer composites exhibit improved mechanical performance. However, only a few studies have investigated the use of biochar in FDM printed parts. One potential application is the use of biochar as a filler in PLA-based composites for FDM printing. The resulting biocomposite could potentially offer improved mechanical performance, reduced environmental impact, and enhanced sustainability. George et al. added coconut shell biochar in powdered form to PLA/polybutylene adipate-co-terephthalate (PBAT) composite, and then this mixer was extruded to form a filament through FDM [22]. When 0.75 wt.% high-quality biochar was added as a filler to polypropylene, the ultimate tensile strength and Young's modulus of 3D-printed biocomposite improved by 46 % and 34 %, respectively [23].

Table 2
Extrusion process temperature for filament manufacturing.

Barrel zone	Feed zone[°C]	Compression zone [°C]	Mixing zone [°C]	Die zone [°C]	Screw speed [RPM]
PLA	195	195	220	210	30
PLA + biochar + PEG	180	185	195	195	20
Cooling	Normal temperature of water				

In the study by Idrees et al. [24], there was a 32 % increase in strength (tensile) with 0.5 % biochar and a 60 % improvement in modulus (tensile) with 5 % biochar in PET (polyethylene terephthalate).

In the current investigation, the effect of incorporating biochar into PLA and the influence of selected process parameters of FDM 3D printing on the mechanical properties of the resulting biocomposites were studied. Biochar was added in various proportions to PLA, and the batches were extruded into FDM filaments of a diameter of 1.75 mm. On the basis of the Taguchi L_{16} experimental design, test specimens were 3D printed. Different mechanical tests were performed as per the standards, and the results were analysed accordingly.

2. Materials and methods

2.1. Materials

Biochar (BC), produced from pyrolysis of rice husk at 600 °C, was provided by Universal Bio-Con Pvt. Ltd., Pune. NaturTech India Ltd., Chennai, provided the Polylactic Acid (PLA): 3D850 granules. Table 1 lists the physical and mechanical parameters of the PLA obtained. To improve the flexibility and printability of the resulting filament, glycol was used as a plasticizer. Polyethylene glycol (PEG) was purchased by Shiv Shakti Trading Corporation, Vadodara.

2.2. Production of biocomposite filament for FDM

The filament manufacturing process consisted of preparing four batches. In the first batch, PLA granules were mixed with 2 % glycol using a batch mixer. In the second batch, PLA granules were blended with 1 % biochar and 2 % glycol. The third and fourth batches involved mixing PLA granules with 3 % and 5 % biochar, respectively, along with 2 % glycol. Each batch was carefully mixed in the batch mixer to achieve a uniform composition. Once the batches were prepared, they were transferred to a single-screw extruder. Table 2 shows the temperature set at different zones. The extruder was set to appropriate parameters, including temperature at 170 °C to 210 °C according to zone in the barrel, screw speed at 20–30 rpm, and die pressure at 2500–3000 PSI, for processing of BC/PLA composite filament. The batches were then heated, melted, and thoroughly mixed within the extruder barrel. The molten PLA composites were extruded through a die, which shaped them into continuous filaments of 1.75 mm diameter. Fig. 1 represents a schematic illustration of the manufacturing Biochar/PLA composite filament for FDM process.

2.3. Process parameters of FDM

According to the literature [1,3,4,9,25], the process parameters utilised in the Fused Deposition Modelling (FDM) technique have a

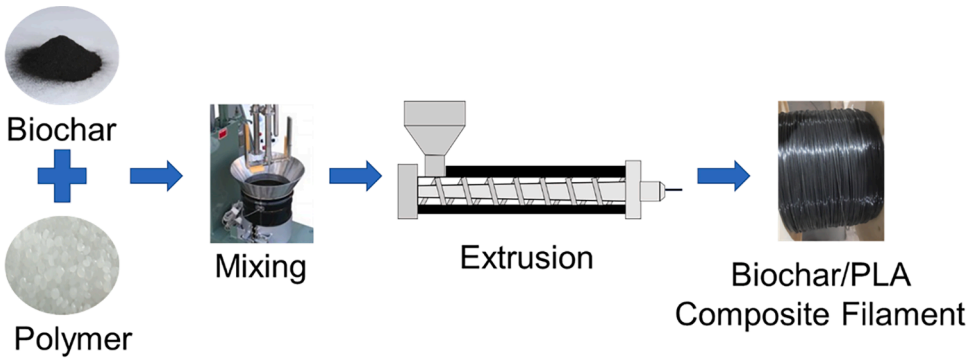

Fig. 1. Illustration of manufacturing Biochar/PLA composite filament for FDM process.

Table 3
3D printing parameters set to constant.

Process parameter of FDM	Settings
Bed temperature	50 °C
Extruder temperature	210 °C
Build orientation	Flat
Printing speed	60 mm/s
Nozzle diameter	0.4 mm

Table 4
Chosen process parameters and corresponding levels in the experimental design.

Parameters	Level 1	Level 2	Level 3	Level 4
% Weight of biochar in the composite *(%WBC)*	0	1	3	5
Layer thickness *(LT)* (mm)	0.1	0.2	0.3	0.4
Raster angle *(RA)* (°)	0	30	45	90
Infill density *(ID)* (%)	40	60	80	100
Pattern	Cubic	Triangle	Octate	Line

significant impact on the mechanical properties of 3D printed products. While some aspects, such as printing speed, may have little effect on mechanical quantities [26], others can be critical. As a result, the aim of this research is to look particularly at the effect of four critical process characteristics, namely the printing pattern, layer thickness, raster angle, and infill density, while leaving the remaining process parameters at their normal settings.

Table 3 lists some of the non-observed constant process parameters.

By focusing on these selected parameters, the study aims to gain a deeper understanding of their individual effects on the mechanical properties of 3D printed items. The printing pattern refers to the specific path followed by the extrusion nozzle during printing, which can impact factors such as strength and surface finish. Layer thickness determines the thickness of each printed layer and can affect the resolution and strength of the final object. The raster angle, which refers to the orientation of the infill pattern, can influence mechanical properties like tensile strength and stiffness. Lastly, infill density, which represents the amount of material filling the internal structure of the object, can significantly impact its strength and weight.

The study intends to provide significant insights into optimising the FDM process to accomplish enhanced mechanical characteristics in 3D printed products by systematically varying and analysing selected process parameters.

2.4. Design of experiments

Table 4 represents the five parameters under investigation and the four levels of variation. The Taguchi design is employed to achieve reliable and robust results, reduce experimentation time, and cost, and gain valuable insights into the factors that have the most significant impact on the response variable. L16 Taguchi orthogonal array was used in this study to examine the effect of selected factors and levels using the software Minitab for statistical analysis. Biochar/PLA composite samples were printed in the configurations shown in Table 5.

Table 5
Taguchi L16 orthogonal array of design of experiment.

Experiment run	% weight of biochar	Layer thickness	Raster angle	Infill density	Pattern
1	0	0.1	0	0.4	Cubic
2	0	0.2	30	0.6	Triangle
3	0	0.3	45	0.8	Octate
4	0	0.4	90	1	Line
5	1	0.1	30	0.8	Line
6	1	0.2	0	1	Octate
7	1	0.3	90	0.4	Triangle
8	1	0.4	45	0.6	Cubic
9	3	0.1	45	1	Triangle
10	3	0.2	90	0.8	Cubic
11	3	0.3	0	0.6	Line
12	3	0.4	30	0.4	Octate
13	5	0.1	90	0.6	Octate
14	5	0.2	45	0.4	Line
15	5	0.3	30	1	Cubic
16	5	0.4	0	0.8	Triangle

2.5. Manufacturing and testing of bio-composite specimen

Ultimaker Cura Software was used for generating G-code for exported CAD models for 3D printing. An FDM-based 3D printer (Smart Maker Dual Z200 by Rio 3D Printers) was used for manufacturing the biochar/PLA composite specimens. The parameters mentioned in Table 3 were set, and as per Table 5, the remaining variables were changed for different runs of the experiments.

Tensile testing was conducted as per the ASTM D638 standards to evaluate the strength and modulus of the FDM printed specimens. To ensure the accuracy and repeatability of the findings, the experiment was carried out three times independently. The specimens of size 165 mm (length), 19 mm (grip section width), 13 mm (gauge section width), and 3.2 mm (thickness) were tightly clamped at a 115 mm distance. On a universal testing machine (Make: Kalpak Instruments and Controls, Pune, India) with a 10 kN load cell capacity, a uniform tensile load was applied with a crosshead speed of 2 mm/min until failure. The data of load vs. displacement was recorded, and accordingly, the tensile strength and tensile modulus were evaluated.

A three-point bending setup was used to perform the flexural test, following ASTM D790 standards. As per ASTM requirements, rectangular specimens of size 127 mm × 12.7 mm × 3.2 mm with a span-to-depth ratio of 16:1 were used. During the bending test, the crosshead speed was 1.3 mm/min with 10 kN load cell capacity. The flexural

Fig. 2. 3D printed biochar/PLA composite specimens for tensile, flexural, and impact test.

Table 6
Mechanical properties observed for the 16 experiment runs.

Experiment run	UTS (MPa)	TM (MPa)	FS (MPa)	FM (MPa)	IS (KJ/m^2)
1	13 ± 2.3	417 ± 06	29 ± 3.5	1083 ± 321	21 ± 1.8
2	23 ± 0.7	566 ± 48	53 ± 0.9	2086 ± 932	25 ± 0.4
3	32 ± 1.9	899 ± 41	66 ± 2.6	2632 ± 430	25 ± 0.3
4	06 ± 2.3	318 ± 12	68 ± 1.7	2123 ± 396	28 ± 3.6
5	23 ± 1.3	792 ± 29	52 ± 0.9	1901 ± 176	38 ± 0.5
6	34 ± 0.6	968 ± 43	60 ± 2.0	2380 ± 493	32 ± 0.8
7	20 ± 1.4	596 ± 16	46 ± 2.1	2392 ± 307	21 ± 1.8
8	27 ± 1.7	750 ± 09	46 ± 1.9	2418 ± 357	23 ± 3.7
9	29 ± 1.2	1004 ± 21	57 ± 0.6	2884 ± 290	32 ± 0.8
10	30 ± 2.6	920 ± 10	60 ± 2.1	2350 ± 595	25 ± 0.2
11	31 ± 3.3	953 ± 53	45 ± 3.1	2511 ± 552	23 ± 3.7
12	27 ± 0.4	802 ± 21	52 ± 1.1	1742 ± 303	23 ± 3.7
13	16 ± 1.1	582 ± 37	36 ± 3.8	2279 ± 735	15 ± 3.6
14	15 ± 0.5	548 ± 04	34 ± 4.4	1621 ± 255	11 ± 3.4
15	36 ± 1.7	1103 ± 36	64 ± 4.8	2452 ± 888	18 ± 4.7
16	23 ± 0.7	826 ± 23	40 ± 2.9	1801 ± 132	19 ± 6.3

modulus and flexural strength were evaluated based on the recorded data of load vs. displacement and equations given in the ASTM standard.

The Izod impact testing machine (International Equipment, Mumbai) was utilised for impact testing in accordance with ASTM D256 standards. The strip shape specimens of dimensions 64 mm (length) × 13 mm (width) × 3.2 mm (thickness) were used for impact testing. Using a motorized notch cutter, a v notch is formed along the width to reduce it to 10.16 mm and 45° angles. The energy absorbed during the fracture of the 3D printed specimen was recorded, and then the impact strength for biochar/PLA composite was evaluated. Fig. 2 shows 3D-printed test specimens for tensile, flexural, and impact testing made by biochar/PLA composite.

3. Results and discussion

3.1. Mechanical properties

Three specimens are printed using an FDM printer and tested for every experimental run. Table 6 shows the mean of each specimen as a representative result for ultimate tensile strength (UTS), tensile modulus (TM), flexural strength (FS), flexural modulus (FM), and impact strength (IS).

3.1.1. Effect of process parameters on tensile properties

Maximum tensile strength (36 MPa) and modulus (1103 MPa) are found at 100 % infill density, 0.3-layer thickness, a 30° raster angle, and a cubic pattern for PLA composite with 5 % biochar (see Table 6). The main effect plots were constructed to analyse the effects of process parameters on tensile strength and tensile modulus to acquire a better understanding of their influence (see Fig. 3). The stress-strain behaviour of 16 FDM-printed test specimens under tensile loading is shown in Fig. 4.

Based on the analysis of variance, all five process parameters were found to have a substantial impact on the tensile strength of the 3D-printed items. The main effect plot further revealed the optimized process parameters for maximizing the tensile strength and tensile modulus. These optimized parameters include an 80 % infill density, a 0.3-layer thickness, a 30° raster angle, and utilizing the Octate pattern for PLA composite with 3 % biochar. A higher infill density results in a denser internal structure, resulting in more material contributing to load transfer during tensile testing. This increases the overall strength of the printed object. Thicker layers tend to provide better interlayer adhesion, enhancing the integrity and strength of the printed item [25]. In the case of tensile modulus, analysis of variance indicated that all the process parameters were significant, but biochar composition was found to be dominant with a 39 % contribution. Within the PLA matrix, the biochar particles might create a network-like structure [27]. This network improves particle-to-particle load transfer, resulting in more efficient stress distribution and load-bearing capability. As a result, the composite material has increased stiffness and tensile modulus. An increase in biochar resulting in an increase in tensile modulus has been observed in various studies [28–31]

3.1.2. Effect of process parameters on flexural properties

A maximum flexural strength of 68 MPa was found for pure PLA, and a maximum flexural modulus of 2884 MPa was obtained for 3 % biochar composition (refer to Table 6). According to the Mean Effect Plot (MEP), the optimum parameters for maximizing flexural strength and flexural modulus were determined. It was found that a layer thickness of 0.3 mm, a biochar content of 3 %, and a 100 % infill density were the key parameters to achieve the highest values for flexural properties (see Fig. 5). Fig. 6 shows the load-displacement behaviour of 16 FDM-printed specimens under flexural testing.

Additionally, the Analysis of Variance (ANOVA) revealed insights into the significance of various process parameters. The effect of the infill pattern was found to be insignificant, suggesting that different patterns did not significantly influence the flexural strength and flexural modulus. Akhil et al. also discovered that in bending tests, all of the infill patterns under investigation exhibit similar relationships for flexural stress and strain [32]. On the other hand, the infill density was identified as the most significant parameter, contributing approximately 52 % to the variation in flexural strength and 44 % to the variation in flexural modulus. Infill acts as a connector linking the top ceiling and floor layers, providing support. As infill density lowers, the reinforcement's ability to bear the load reduces, which results in lower flexural properties [33].

3.1.3. Effect of process parameters on impact properties

The impact strength of the 3D printed composite reached its

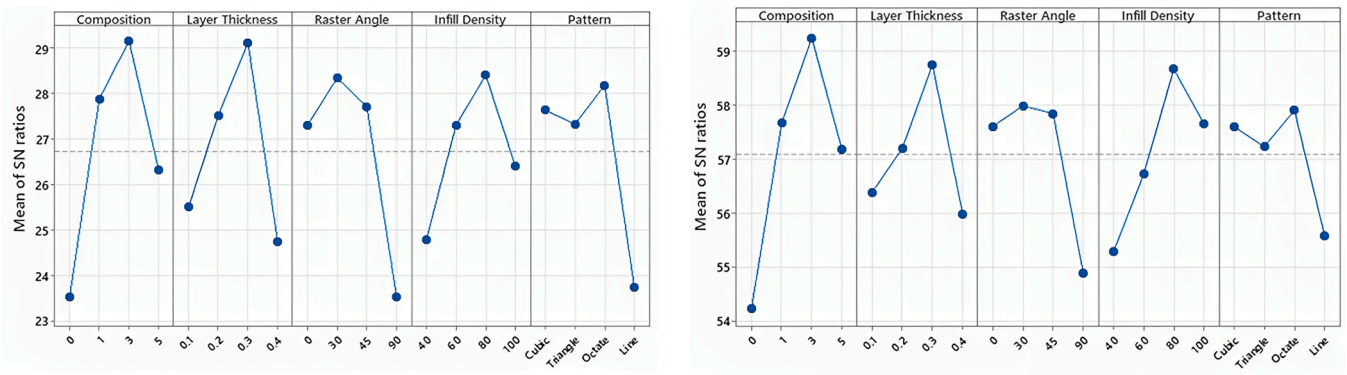

Fig. 3. Main effects plot for (a) tensile strength and (b) tensile modulus.

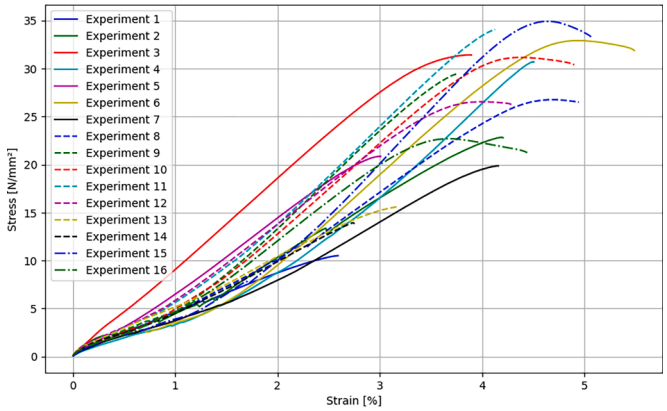

Fig. 4. Stress-Strain behaviour of 16 FDM-printed biocomposite experiments.

maximum value of 38 KJ/m^2 when using a 1 % biochar composition with an 80 % infill density, as indicated in Table 6. The MEP for the Signal-to-Noise (SN) ratio of impact strength, shown in Fig. 7, provides further insights. The analysis of variance (ANOVA) revealed that layer thickness, raster angle, and infill pattern had an insignificant effect on impact strength, while the composition emerged as the most dominant process parameter, contributing 62 % towards the observed variations.

The results as per Table 5 show an increase of 52 % in impact strength of 3D printed composites with 1 % biochar content compared to pure PLA. The reason for this was the increase in interfacial bonding of biochar with PLA matrix [34]. It has been observed that there was a decrease in impact strength with an increase in the biochar content. This is due to an increase in the voids between the biochar filler and PLA matrix, which diminishes the composites' ability to absorb energy. This was also reported by Shahar et al. [35].

3.2. Multi-criteria decision analysis using TOPSIS

The most popular option among multicriteria decision-making models and multiple attribute models for the most desirable option has been TOPSIS. Using TOPSIS, it is possible to choose the ideal set of parameters. This is determined by the selection criteria, which include impact strength, flexural strength, flexural modulus, and tensile strength. 16 tests with various parameter levels are obtained by the Taguchi experimental design. These experiments are ranked using TOPSIS based on the results of each test's performance output. It requires some steps to be followed as below:

Step 1 – Create the decision matrix

$C_1 \quad C_2 \ldots\ldots \quad C_3$

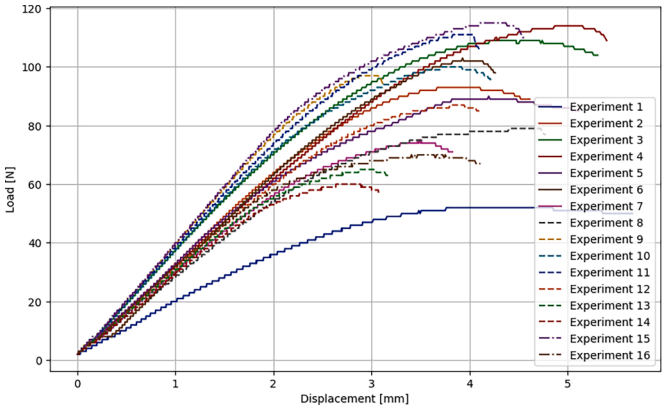

Fig. 6. Load-displacement behaviour of 16 flexural test experiments.

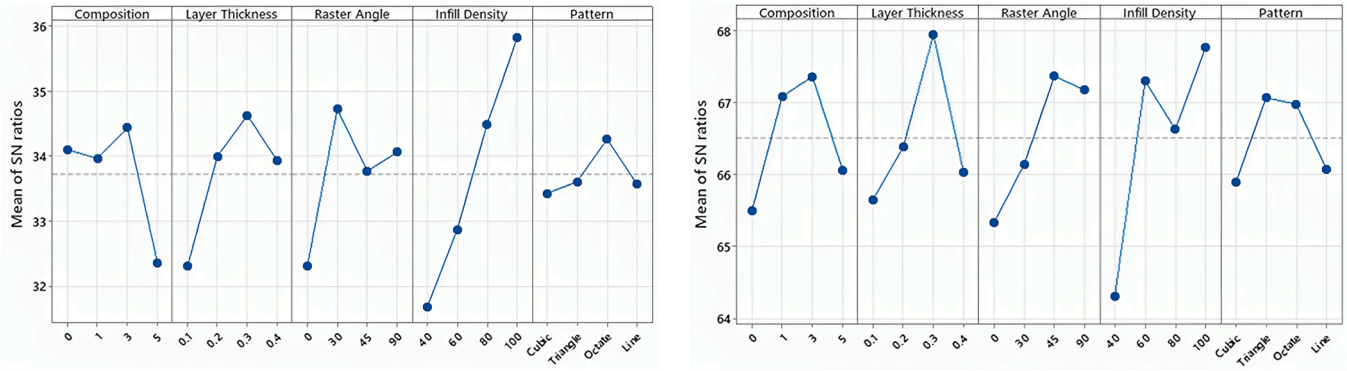

Fig. 5. Main effects plot for (a) flexural strength and b) flexural modulus.

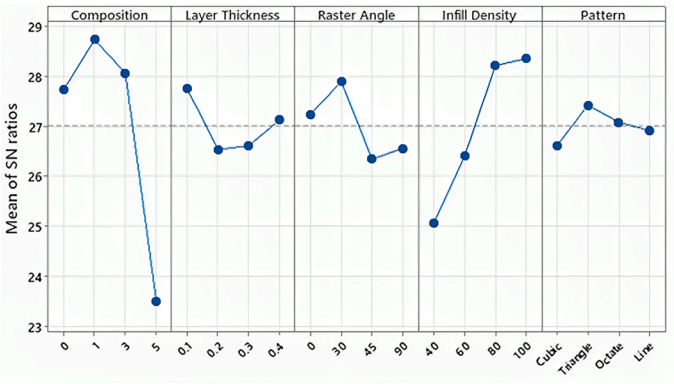

Fig. 7. Main effects plot for impact strength.

$$D = \begin{matrix} A_1 \\ A_2 \\ A_m \end{matrix} \begin{bmatrix} X_{11} & X_{12}\ldots\ldots & X_{1n} \\ X_{21} & X_{22}\ldots\ldots & X_{2n} \\ X_{m1} & X_{m2}\ldots\ldots & X_{mn} \end{bmatrix}$$

where A_1, $A2$, A_m are the alternatives, C_1, C_2,…, C_n are the criteria based on which ranking is done. X_{ij} is the qualification of the alternative A_i with respect to the criterion C_j, and w_j is the weight of the criterion C_j.

Step 2: Determination of normalized decision matrix

$$n_{ij} = \frac{x_{ij}}{\sqrt{\sum_{i-1}^{m} x_{ij}^2}}$$

where, $i = 1, 2,\ldots, m$, $j = 1, 2,\ldots, n$.

Step 3: Determination of weighted normalized decision matrix, and weighted normalized value. Equal weightage is assigned for all the parameters.

$$v_{ij} = r_{ij} \times w_j$$

where, w_j is the relative weight of the j_{th} criterion.

Step 4: Calculate the positive ideal and negative ideal solutions

$$A^{\pm} = \left\{ \left(\max v_{ij} \middle| \, j \in \Omega_b \right), \ \left(\min v_{ij} \middle| \, j \in \Omega_c \right) \right\} = \left\{ v_j^{\pm} \middle| j = 1, \ 2, \ \ldots, \ n \right\}$$

$$A^{-} = \left\{ \left(\max v_{ij} \middle| \, j \in \Omega_b \right), \ \left(\min v_{ij} \middle| \, j \in \Omega_c \right) \right\} = \left\{ v_j^{-} \middle| j = 1, \ 2, \ \ldots, \ n \right\}$$

where, Ω_c and Ω_c are the sets of benefit criteria/attributes and cost criteria/attributes, respectively.

Step 5: Determine the separation from positive and negative ideal solution as below:

$$d_i^{\pm} = \sqrt{\sum_{j=1}^{m} \left(v_{ij} - v_j^{\pm} \right)^2}, \ j = 1, \ 2, \ \ldots\ldots, \ \mathrm{n}$$

$$d_i^{-} = \sqrt{\sum_{j=1}^{m} \left(v_{ij} - v_j^{-} \right)^2}, \ j = 1, \ 2, \ \ldots\ldots, \ \mathrm{n}$$

Table 7
Ranking of experiments using TOPSIS.

	Decision matrix (average)					Normalised decision matrix					Weight normalised decision matrix					Closeness to ideal solution		Ranking of experiments	
Expt. no.	UTS (MPa)	TM (MPa)	FM (MPa)	FS (MPa)	IS (KJ/m^2)	UTS	TM	FM	FS	IS	UTS	TM	FM	FS	IS	Si±	Si-	Pi	Rank
1	13	417	1083	29	21	0.1246	0.1393	0.1225	0.1370	0.2149	0.0249	0.0279	0.0245	0.0274	0.0430	0.0906	0.0265	0.2260	**16**
2	23	566	2086	53	25	0.2283	0.1807	0.2361	0.2569	0.2579	0.0457	0.0361	0.0472	0.0514	0.0516	0.0547	0.0585	0.5165	**10**
3	32	899	2632	66	25	0.3199	0.2872	0.2979	0.3213	0.2579	0.0640	0.0574	0.0596	0.0643	0.0516	0.0302	0.0874	0.7431	**3**
4	06	318	2123	68	28	0.0570	0.1014	0.2403	0.3296	0.2793	0.0114	0.0203	0.0481	0.0659	0.0559	0.0823	0.0567	0.4081	**13**
5	23	792	1901	52	38	0.2246	0.2528	0.2151	0.2496	0.3868	0.0449	0.0506	0.0430	0.0499	0.0774	0.0424	0.0775	0.6461	**7**
6	34	968	2380	60	32	0.3326	0.3091	0.2694	0.2896	0.3224	0.0665	0.0618	0.0539	0.0579	0.0645	0.0212	0.0917	0.8119	**1**
7	20	596	2392	46	21	0.1949	0.1902	0.2707	0.2199	0.2149	0.0390	0.0380	0.0541	0.0440	0.0430	0.0619	0.0519	0.4558	**12**
8	27	750	2418	46	23	0.2641	0.2394	0.2737	0.2204	0.2364	0.0528	0.0479	0.0547	0.0441	0.0473	0.0481	0.0658	0.5776	**8**
9	29	1004	2884	57	32	0.2898	0.3207	0.3264	0.2764	0.3224	0.0580	0.0641	0.0653	0.0553	0.0645	0.0218	0.0915	0.8072	**2**
10	30	920	2350	60	25	0.2953	0.2939	0.2660	0.2920	0.2579	0.0591	0.0588	0.0532	0.0584	0.0516	0.0336	0.0803	0.7044	**4**
11	31	953	2511	45	23	0.3080	0.3043	0.2842	0.2165	0.2364	0.0616	0.0609	0.0568	0.0433	0.0473	0.0407	0.0783	0.6577	**6**
12	27	802	1742	52	23	0.2616	0.2562	0.1971	0.2491	0.2364	0.0523	0.0512	0.0394	0.0498	0.0473	0.0503	0.0634	0.5575	**9**
13	16	582	2279	36	15	0.1584	0.1746	0.2579	0.1731	0.1504	0.0317	0.0349	0.0516	0.0346	0.0301	0.0786	0.0385	0.3289	**14**
14	15	548	1621	34	11	0.1449	0.1748	0.1834	0.1638	0.1075	0.0290	0.0350	0.0367	0.0328	0.0215	0.0895	0.0265	0.2281	**15**
15	36	1103	2452	64	18	0.3528	0.3522	0.2775	0.3106	0.1827	0.0706	0.0704	0.0555	0.0621	0.0365	0.0421	0.0917	0.6851	**5**
16	23	826	1801	40	19	0.2300	0.2639	0.2039	0.1906	0.1934	0.0460	0.0528	0.0408	0.0381	0.0387	0.0615	0.0541	0.4680	**11**

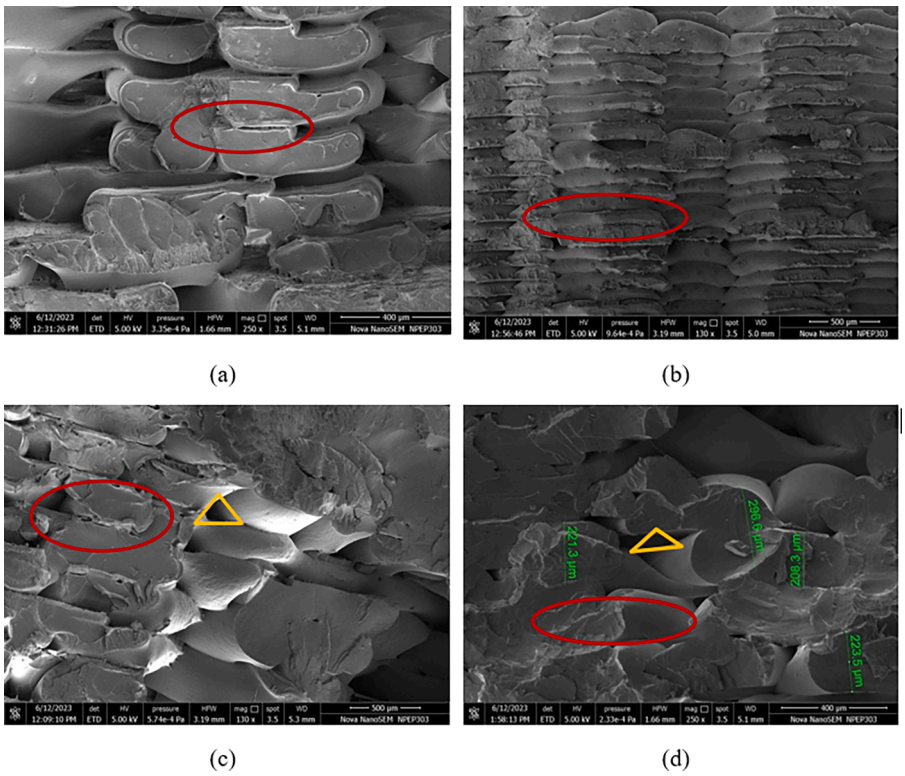

Fig. 8. SEM Morphology of tensile fractured specimen of experiment run number (a) 6, (b) 9, (c) 3 and (d) 10.

Step 6: Determine the relative closeness to the ideal solution and ranking of experiments.

$$cl_i^{\pm} = \frac{d_i^{-}}{d_i^{\pm} \pm d_i^{-}}$$

The decision matrix, normalization matrix, weight-normalized matrix, relative closeness value, and ranking are shown in Table 6. It is observed that experiment no. 6 is ranked 1 as per the TOPSIS. The 1 wt. % biochar with 100 % infill and 0° raster angles are the best process parameters for 3D printing of the biochar PLA composite. The second ranked experiment is 9, which has 3 wt.% biochar with 100 % infill and 45° raster angles. The third ranked experiment is 3, which has 0 wt.% biochar with 80 % infill and 45° raster angles. From the first 3 ranks, it can be concluded that 1 and 3 wt.% of biochar in PLA is suitable for obtaining optimized properties, whereas the experiments having 5 wt.% are not ranked in the top (Table 7).

3.3. Morphology of tensile fractured specimen

As per TOPSIS multi-criterion decision-making, the top four experiment runs are experiments no. 6, 9, 3, and 10. Fig. 8 depicts the fractured cross-sectional surface morphology of tensile specimens from these four tests at a resolution of 500 µm. The surface morphology of the printed specimens, as visible in Fig. 8, offers clear visual confirmation of the selected process parameters detailed in Table 5, such as the raster angle and layer thickness. Fig. 8(a) shows that each layer of a 3D-printed object is precisely aligned and does not show any signs of distortion like swelling, warping, or separation. The influence of these factors is evident in the outcomes, with Experiment 6 achieving the highest tensile strength (TS) at 34 MPa. Experiment 9, on the other hand, yielded a maximum tensile modulus (TM) of 1004 MPa. This high value of TM is likely attributed to the combination of a minimal layer thickness of 0.1 mm and a higher weight percentage of biochar (3 %) used in this experiment. The use of 100 % infill density can be attributed to the increased TS and TM reported in Experiments 6 and 9, compared to Experiments 3 and 10. Experiments with an infill density of 80 %, on the other hand, exhibited a visible gap between layers, as indicated by the yellow triangles in Fig. 8(c) and (d). This difference led to a reduction in both TS and TM for the biochar/PLA composite.

4. Conclusion

The successful extrusion of 3D printing filament made from rice husk biochar/PLA biocomposite has been achieved, making it suitable for fused deposition modelling (FDM) applications. The addition of biochar resulted in an increase in tensile strength, tensile modulus, and flexural modulus of 89 %, 100 %, and 45 %, respectively, compared to 3D-printed PLA. This indicates that the 3D-printed biochar/PLA biocomposite can be well-suited for applications requiring increased stiffness. Furthermore, the impact strength of the biocomposite showed a substantial increase of ~52 % compared to neat PLA at 1 wt.% loading of biochar. The analysis of variance (ANOVA) revealed that the % weight of biochar in the composite had a significant effect on both tensile and impact properties. It was found that, up to a point, the addition of biochar resulted in improved tensile and impact performance. Additionally, infill density had a substantial influence on the flexural properties of the 3D-printed biocomposites. The effect of the infill pattern was found to be insignificant on the mechanical properties of the biocomposites. The mechanical performance was ranked according to the outcome of each test by the multicriteria decision-making model TOPSIS, and experiment number 6 was given rank one. Finally, including biochar in FDM printed parts has the potential to provide significant benefits in terms of mechanical performance and sustainability. Further research is required to optimize the printing parameters and biochar content to attain the desirable characteristics. The development of biochar reinforced FDM printed parts may offer new avenues for environmentally friendly and

high-performance engineering uses.

Declaration of Competing Interest

The authors declare the following financial interests/personal relationships which may be considered as potential competing interests:

Oisik Das reports article publishing charges was provided by Department of Civil, Environmental and Natural Resources Engineering, Lulea University of Technology, Lulea, Sweden.

Data availability

Data will be made available on request.

References

[1] A.K. Sood, R.K. Ohdar, S.S. Mahapatra, Parametric appraisal of mechanical property of fused deposition modelling processed parts, Mater. Des. 31 (2010) 287–295, https://doi.org/10.1016/j.matdes.2009.06.016.

[2] S. Bhagia, K. Bornani, R. Agarwal, A. Satlewal, J. Ďurkovič, R. Lagaňa, M. Bhagia, C.G. Yoo, X. Zhao, V. Kunc, Y. Pu, S. Ozcan, A.J. Ragauskas, Critical review of FDM 3D printing of PLA biocomposites filled with biomass resources, characterization, biodegradability, upcycling and opportunities for biorefineries, Appl. Mater. Today 24 (2021), https://doi.org/10.1016/j.apmt.2021.101078.

[3] A. Rodríguez-Panes, J. Claver, A.M. Camacho, The influence of manufacturing parameters on the mechanical behaviour of PLA and ABS pieces manufactured by FDM: a comparative analysis, Materials 11 (2018), https://doi.org/10.3390/ma11081333.

[4] H. Chokshi, D.B. Shah, K.M. Patel, S.J. Joshi, Experimental investigations of process parameters on mechanical properties for PLA during processing in FDM, Adv. Mater. Process. Technol. 8 (2022) 696–709, https://doi.org/10.1080/2374068X.2021.1946756.

[5] R.A. Mensah, D.A. Edström, O. Lundberg, V. Shanmugam, L. Jiang, X. Qiang, M. Försth, G. Sas, M. Hedenqvist, O. Das, The effect of infill density on the fire properties of polylactic acid 3D printed parts: a short communication, Polym. Test. 111 (2022), https://doi.org/10.1016/j.polymertesting.2022.107594.

[6] A.R. Prajapati, H.K. Dave, H.K. Raval, Effect of fiber volume fraction on the impact strength of fiber reinforced polymer composites made by FDM process. Mater Today Proc, Elsevier Ltd, 2021, pp. 2102–2106, https://doi.org/10.1016/j.matpr.2020.12.262.

[7] S. Antony, A. Cherouat, G. Montay, Fabrication and characterization of hemp fibre based 3D printed honeycomb sandwich structure by FDM process, Appl. Compos. Mater. 27 (2020) 935–953, https://doi.org/10.1007/s10443-020-09837-z.

[8] S.A. Hinchcliffe, K.M. Hess, W.V. Srubar, Experimental and theoretical investigation of prestressed natural fiber-reinforced polylactic acid (PLA) composite materials, Compos. Part B 95 (2016) 346–354, https://doi.org/10.1016/j.compositesb.2016.03.089.

[9] Y.E. Belarbi, S. Guessasma, S. Belhabib, F. Benmahiddine, A.E.A. Hamami, Effect of printing parameters on mechanical behaviour of pla-flax printed structures by fused deposition modelling, Materials 14 (2021) 1–17, https://doi.org/10.3390/ma14195883.

[10] V. Gigante, L. Aliotta, I. Canesi, M. Sandroni, A. Lazzeri, M.B. Coltelli, P. Cinelli, Improvement of interfacial adhesion and thermomechanical properties of PLA based composites with wheat/rice bran, Polymers (Basel) 14 (2022), https://doi.org/10.3390/polym14163389.

[11] V. Shanmugam, S.N. Sreenivasan, R.A. Mensah, M. Försth, G. Sas, M.S. Hedenqvist, R.E. Neisiany, Y. Tu, O. Das, A review on combustion and mechanical behaviour of pyrolysis biochar, Mater. Today Commun. 31 (2022), https://doi.org/10.1016/j.mtcomm.2022.103629.

[12] O. Das, A.K. Sarmah, D. Bhattacharyya, A novel approach in organic waste utilization through biochar addition in wood/polypropylene composites, Waste Manag. 38 (2015) 132–140, https://doi.org/10.1016/j.wasman.2015.01.015.

[13] G. Ahmetli, S. Kocaman, I. Ozaytekin, P. Bozkurt, Epoxy composites based on inexpensive char filler obtained from plastic waste and natural resources, Polym. Compos. 34 (2013) 500–509, https://doi.org/10.1002/pc.22452.

[14] M.R. Snowdon, A.K. Mohanty, M. Misra, A study of carbonized lignin as an alternative to carbon black, ACS Sustain. Chem. Eng. 2 (2014) 1257–1263, https://doi.org/10.1021/sc500086v.

[15] S. Kane, C. Ryan, Biochar from food waste as a sustainable replacement for carbon black in upcycled or compostable composites, Compos. Part C 8 (2022), https://doi.org/10.1016/j.jcomc.2022.100274.

[16] C.C. Huang, C.W. Chang, K. Jahan, T.M. Wu, Y.F. Shih, Effects of the grapevine biochar on the properties of PLA composites, Materials 16 (2023), https://doi.org/10.3390/ma16020816.

[17] M. Zouari, D.B. Devallance, L. Marrot, Effect of biochar addition on mechanical properties, thermal stability, and water resistance of hemp-polylactic acid (PLA) composites, Materials 15 (2022), https://doi.org/10.3390/ma15062271.

[18] S. Kane, E. Van Roijen, C. Ryan, S. Miller, Reducing the environmental impacts of plastics while increasing strength: biochar fillers in biodegradable, recycled, and fossil-fuel derived plastics, Compos. Part C 8 (2022), https://doi.org/10.1016/j.jcomc.2022.100253.

[19] A. Pudełko, P. Postawa, T. Stachowiak, K. Malińska, D. Dróżdż, Waste derived biochar as an alternative filler in biocomposites—Mechanical, thermal and morphological properties of biochar added biocomposites, J. Clean. Prod. 278 (2021), https://doi.org/10.1016/j.jclepro.2020.123850.

[20] K. Aup-Ngoen, M. Noipitak, Effect of carbon-rich biochar on mechanical properties of PLA-biochar composites, Sustain. Chem. Pharm. 15 (2020), https://doi.org/10.1016/j.scp.2019.100204.

[21] Q. Zhang, M.U. Khan, X. Lin, H. Cai, H. Lei, Temperature varied biochar as a reinforcing filler for high-density polyethylene composites, Compos. Part B 175 (2019), https://doi.org/10.1016/j.compositesb.2019.107151.

[22] J. George, D. Jung, D. Bhattacharyya, Improvement of electrical and mechanical properties of PLA/PBAT composites using coconut shell biochar for antistatic applications, Appl. Sci. (Switzerland) 13 (2023), https://doi.org/10.3390/app13020902.

[23] Z. Mohammed, S. Jeelani, V. Rangari, Effective reinforcement of engineered sustainable biochar carbon for 3D printed polypropylene biocomposites, Compos. Part C 7 (2022), https://doi.org/10.1016/j.jcomc.2021.100221.

[24] M. Idrees, S. Jeelani, V. Rangari, Three-dimensional-printed sustainable biochar-recycled PET composites, ACS Sustain. Chem. Eng. 6 (2018) 13940–13948, https://doi.org/10.1021/acssuschemeng.8b02283.

[25] M.D. Zandi, R. Jerez-Mesa, J. Lluma-Fuentes, J. Jorba-Peiro, J.A. Travieso-Rodriguez, Study of the manufacturing process effects of fused filament fabrication and injection molding on tensile properties of composite PLA-wood parts, Int. J. Adv. Manuf. Technol. 108 (2020) 1725–1735, https://doi.org/10.1007/s00170-020-05522-4.

[26] J.D. Kechagias, S. Zaoutsos, D. Chaidas, Parameter design of PLA/wood fused filament fabrication using Taguchi optimization methodology, (2021). https://doi.org/10.21203/rs.3.rs-1074258/v1.

[27] M. Bartoli, R. Arrigo, G. Malucelli, A. Tagliaferro, D. Duraccio, Recent advances in biochar polymer composites, Polymers (Basel). 14 (2022), https://doi.org/10.3390/polym14122506.

[28] R. Arrigo, M. Bartoli, G. Malucelli, Poly(lactic acid)-biochar biocomposites: effect of processing and filler content on rheological, thermal, and mechanical properties, Polymers (Basel) 12 (2020), https://doi.org/10.3390/POLYM12040892.

[29] O. Das, R.A. Mensah, K.B.N. Balasubramanian, V. Shanmugam, M. Försth, M. S. Hedenqvist, P. Rantuch, J. Martinka, L. Jiang, Q. Xu, R.E. Neisiany, C.F. Lin, A. Mohanty, M. Misra, Functionalised biochar in biocomposites: the effect of fire retardants, bioplastics and processing methods, Compos. Part C 11 (2023), https://doi.org/10.1016/j.jcomc.2023.100368.

[30] R.A. Mensah, A. Vennström, V. Shanmugam, M. Försth, Z. Li, A. Restas, R. E. Neisiany, D. Sokol, M. Misra, A. Mohanty, M. Hedenqvist, O. Das, Influence of biochar and flame retardant on mechanical, thermal, and flammability properties of wheat gluten composites, Compos. Part C 9 (2022), https://doi.org/10.1016/j.jcomc.2022.100332.

[31] T. Perroud, V. Shanmugam, R.A. Mensah, L. Jiang, Q. Xu, R.E. Neisiany, G. Sas, M. Försth, N.K. Kim, M.S. Hedenqvist, O. Das, Testing bioplastic containing functionalised biochar, Polym. Test. 113 (2022), https://doi.org/10.1016/j.polymertesting.2022.107657.

[32] V.M. Akhil, S.L. Aravind, R. Kiran, S. S P, S. Mohan, Experimental investigations on the effect of infill patterns on PLA for structural applications, Mater. Today Proc. (2022), https://doi.org/10.1016/j.matpr.2022.10.292.

[33] R. Chen, L. Baich, J. Lauer, D.G. Senesky, G. Manogharan, Manufacturing letters effects of part orientation, printer selection, and infill density on mechanical properties and production cost of 3D printed flexural specimens, 2022. www.sciencedirect.com.

[34] S.H. Kamarudin, L.C. Abdullah, M.M. Aung, C.T. Ratnam, E.R. Jusoh Talib, A study of mechanical and morphological properties of PLA based biocomposites prepared with EJO vegetable oil based plasticiser and kenaf fibres, Mater. Res. Express 5 (2018), https://doi.org/10.1088/2053-1591/aabb89.

[35] F.S. Shahar, M.T. Hameed Sultan, S.N.A. Safri, M. Jawaid, A.R. Abu Talib, A. A. Basri, A.U. Md Shah, Fatigue and impact properties of 3D printed PLA reinforced with kenaf particles, J. Mater. Res. Technol. 16 (2022) 461–470, https://doi.org/10.1016/j.jmrt.2021.12.023.